climate

MDPI

Article

Downscaling of Future Temperature and Precipitation Extremes in Addis Ababa under Climate Change

Getnet Feyissa [1,*], Gete Zeleke [1], Woldeamlak Bewket [2] and Ephrem Gebremariam [1]

[1] EiABC, Addis Ababa University, P.O. Box 518, 1000 Addis Ababa, Ethiopia; gete_2004@yahoo.com (G.Z.); ephrem.gebremariam@eiabc.edu.et (E.G.)
[2] Department of Geography and Environmental Studies, Addis Ababa University, 1000 Addis Ababa, Ethiopia; woldebewket@gmail.com
* Correspondence: getyonani@yahoo.com

Received: 30 April 2018; Accepted: 20 June 2018; Published: 28 June 2018

Abstract: One of the recent advances in climate science research is the development of global general circulation models (GCMs) to simulate changes in climatic elements of the present and future, which helps us to determine consequences earlier and prepare for necessary adaptation measures. However, it is difficult to apply the raw data of GCMs at a local scale, such as the urban scale, without downscaling due to coarse resolution. This study, therefore, statistically downscaled daily maximum temperature, minimum temperature, and precipitation in 30-year intervals from the second generation of the Earth System Model (CanESM2) and Coupled Global Climate Model (CGCM3) under two Representative Concentration Pathways (RCP) Scenarios (RCP4.5 and RCP8.5) and two Special Report Emission Scenarios (SRES), A1B and A2, to examine future changes and their extremes. Two representative meteorological stations (Entoto at high elevation and Addis Ababa at downtown and medium elevation) were selected for model calibration and validation in the Statistical Downscaling Model (SDSM). Twelve core temperature and precipitation indices were selected to assess temperature changes and precipitation extremes. For the largest changes the results showed that the maximum temperature increases were in the range of 0.9 °C (RCP4.5) in 2020 to 2.1 °C (CGCM3A2) in 2080 at Addis Ababa Observatory. The minimum temperature is projected to increase by 0.3 °C (RCP4.5) in 2020 and 1.0 °C in 2080 (CGCM3A1B). While the changes in maximum temperature are lower at Entoto station compared to Addis Ababa Observatory, the highest minimum temperature change is projected at Addis Ababa Observatory, which ranges from 0.25 °C in the 2020s to 1.04 °C in 2080 according to the CGCM3 model. Except for the coldest nights (TNn), the mean temperature and other temperature indices will continue to increase to the end of this century. The highest precipitation change is projected by CGCM3A2 and CanESM2 RCP8.5 at an increase of about 11.8% and 16.62% by 2080. The highest total precipitation increase is 29% (RCP4.5) in winter and 20.9% (RCP8.5) in summer by 2080. There is high interseasonal variability in changes of extreme events. The topographic role will diminish in influence on the air temperature distribution due to the high rate of urbanization. The rise in temperature will exacerbate the urban heat highland effects in warm seasons and an increase in precipitation is expected along with a possible risk of flooding due to a low level of infrastructure development and a high rate of urbanization.

Keywords: climate change; extreme events; general circulation models; RCP scenarios; SRES scenarios; Statistical Downscaling Model

1. Introduction

Scientists have reached a consensus that the global annual average temperature is likely to be 2 °C above pre-industrial levels by 2050, and a 2 °C warmer world will experience more intense

rainfall and more frequent and more intense droughts, floods, heat waves, and other extreme weather events [1–3]. The year 2017 demonstrates up-to-date evidence for climate change as it was the warmest year on record for the global ocean [4]. It is well accepted that climate change will have a far more detrimental effect on developing countries compared to developed countries, mainly because the capacity to respond to such changes is lower in developing countries. Moreover, it seems clear that vulnerability to climate change is closely related to poverty, as the poor are least able to respond to climatic stimuli [5].

Regionally in East Africa, studies indicate that in countries like Burundi, Kenya, Sudan, and Tanzania people are badly hit by the impacts of climate change [6,7]. In Ethiopia in the last few decades, high temperature values were recorded in different parts of the country. The various General Circulation Model (GCM) results also suggest that future climatic change climatic elements will be significant. For instance, the average future change for the whole of Ethiopia for a 30-year period with A2 emissions shows warming in all four seasons in all regions, with annual warming in Ethiopia of 1.2 °C with a range of 0.7–2.3 °C by the 2020s, and by 2.2 °C with a range of 1.4–2.9 °C by the 2050s [8]. So far, some studies have predicted long-term future climate change situations that could prevail up until the end of this century in Ethiopia [9].

The models in the ensemble are broadly consistent, indicating increases in total precipitation occurring in 'heavy' events, and increases in the magnitude of one-day maxima and five-day rainfall maxima [9]. In Kenya, Ethiopia, and Somalia, climate-related extremes have been the dominant trigger of natural disasters [10]. Overall, warm days and nights are projected to become more frequent in the entire Great Horn of Africa, while the occurrence of cold nights is likely to decrease [11].

The results of the temperature and precipitation record obtained above on a large scale are either from the average of meteorological observations or from general circulation models. General circulation models are a tool to understand the climatic conditions of the past and future [12]. In order to use general circulation model results to study the impact of climate change on a local scale, it is common to downscale and bring the results into the finest resolution. In addition to the obtained fine resolution of the data, downscaling has the ability to identify and analyze extreme events [13], which are the points of emphasis when we study urban climate.

Typical definitions of weather and climate extremes consider either the maximum value during a specified time interval (such as a season or year), or instances of exceeding a threshold (the "peaks-over-threshold" [POT], in which universal rather than local thresholds are frequently applied). The IPCC defines extremes as 1–10% of the largest or smallest values of an extreme value distribution for a given period [14]. An extreme weather or climate occurrence is usually defined as one that has extreme values for certain important meteorological variables above (or below) a given pre-existing high threshold near the upper (or lower) climaxes of the range of detected standards of the variable [14].

Changes in climate extremes and their impacts on the natural physical environment were examined by the Intergovernmental Panel on Climate Change [2]. Climate change has the potential to change the intensity and frequency of extremes. More severe climate change can cause dramatic impacts with unpredictable consequences. Therefore, the projection of climate extremes is critical information that is needed to assess the impact of potential climate change on human beings and on the natural environment. Such information also helps with long-term planning at both regional and national levels for mitigation and adaptation strategies because it opens up a space for a set of potential responses [15]. While extreme climate events are generally multifaceted phenomena, the present study, in particular, discusses climate extremes based on daily temperature and precipitation, such as the hottest or coldest day of the year, heavy precipitation events, and dry spells [16].

In Ethiopia, we have explored various downscaling applications and their potential to detect climate change impacts in agricultural and hydrological applications. Some of these applications include statistical downscaling for daily temperature and rainfall in South Wollo [17], the study of future changes in climate parameters in Amhara Regional State [18], future climate studies in northwestern Ethiopia for assessing the hydrological response of the Gilgel Abay River to climate

change in the Lake Tana Basin [19], and the climate change impact on the Geba Catchment in Northern Ethiopia [20]. However, applications of statistical downscaling of general circulation models for the largest cities in Ethiopia have not been undertaken. It is important to use the downscaled results of GCMs to assess future projections and to identify adaptation measures, as recently explored in some large East and North African cities [21,22]. Only a few studies are available for Addis Ababa, which differ in method and temporal scale from this study [23,24].

Some environmental problems like high temperature and extreme rainfall, which results in flooding in Addis Ababa, could be signals of climate change [25]. In the future, flooding problems may also become much more common due to the poor urban storm water management system and due to climate change-induced extreme precipitation events, as observed from models in which precipitation is expected to increase in the future at the highest rate, creating additional problems. Fast urbanization, marked by high-rise buildings in the city, contributes to the occurrence of climate change. When these local conditions meet with the global temperature rise conditions, the environmental quality and thermal comfort of the residents will be affected. The impact of the urbanization-driven land use/cover change has resulted in a notable urban heat island [26].

In order to fill in the gaps related to temporal and spatial resolution using recent scenarios and obtain data to help decision makers fulfill the objectives set for Ethiopia's climate-resilient green economy, the priority has to be given to quantifying the amount and intensity of changes in climate variables and their variations for the 21st century. Therefore the main aim of this study is to statistically downscale the future daily maximum temperature, daily minimum temperature, and precipitation, as well as the statistics of extreme events, for the early identification of the possible associated impacts and to set adaptation priorities. The downscaled results under different scenarios could be considered in environmental policy formulation and urban planning processes in Ethiopia.

2. Materials and Methods

2.1. Description of the Study Area

Addis Ababa is found between 8°50′ N to 9°5′ N and 38°38′ E to 38°54′ E. It is the capital and the largest city of Ethiopia, with a total projected population of 3.44 million people in 2017. The administration of the city is divided into 10 sub-cities. Addis Ababa is home to 25% of the urban population in Ethiopia and is one of the fastest growing cities in Africa. It is the growth engine for Ethiopia and a major pillar in the country's vision to become a middle-income, carbon-neutral, and resilient economy by 2025. The city alone currently contributes approximately 50% to the national Gross Domestic Product, highlighting its strategic role within the overall economic development of the country [27].

The city is located in the central highlands of Ethiopia, covering an area of about 527 km^2 with an average elevation of 2600 m above mean sea level (asl). The altitude range extends from the highest peak at Mount Entoto, which is 3041 m high, to 2051 m above mean sea level at the lower part of the Akaki plain. The average maximum temperature for Addis Ababa over the last 60 years was 22.9 °C and the average minimum temperature was 10.2 °C. Minimum and maximum temperatures show increasing trends from 1951 to 2002 of 0.4 °C per decade and 0.2 °C per decade, respectively; however, there was no major shift in annual and seasonal rainfall during the period 1898–2002 [28]. The average annual rain fall for Addis Ababa is 1184 mm. The wet season is from June to mid-September. The urban area is endowed with three major rivers: Kebena, Little Akaki, and Big Akaki, as well as numerous small streams. The population density varies between sub-cities. The highest density is in Addis Ketema sub-city (37,215 persons per square kilometer). The lowest density is in Akaki Kality sub-city (1832 p/sk.km). All the sub-cities in the downtown have a high population density compared to sub-cities found in peripheral areas. A fast rate of urban expansion is occurring, and built-up areas are rapidly increasing in Addis Ababa [29]. The study area is presented in Figure 1.

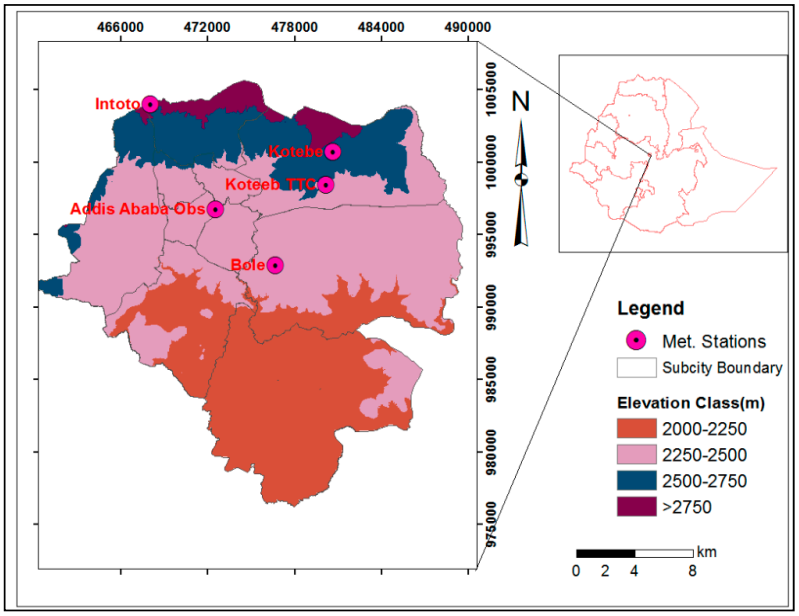

Figure 1. Study area.

2.2. Data Description

The daily observed maximum temperature, minimum temperature and precipitation data from National Meteorological Service Agency of Ethiopia were used for model calibration and validation in SDSM. Of the five meteorological stations with temperature and precipitation records in the city, two stations have been selected based on having complete data and good location representation. Addis Ababa station (9°0′36″ E, 38° 26′ 24″ N, altitude 2386 m) represents the urban center (downtown), while Entoto station (9°3′0″ E, 38°25′48″ N, altitude 2903 m) represents the suburban (peripheral area). Data from 1971–1985 were used for model calibration and from 1986–2000 for model validation at Addis Ababa Observatory. At Entoto station data from 1989–1998 were used for model calibration and 1999–2005 for model validation. The difference in the baseline year is based on the availability of the baseline data in the study area.

All the predictor data have been obtained from a Canadian climate data and scenarios website (http://climate-scenarios.canada.ca).

The general circulation models used in the analyses were:

i. National Center of Environmental Prediction (NCEP): The National Centers for Environmental Prediction (NCEP) National Center for Atmospheric Research (NCAR) reanalysis (NCEPR) project was designed to provide homogenized (gridded) records of atmospheric fields, to support climate research by assimilating data from multiple sources with modeled short-range forecasts [30]. The coherence, accessibility, and completeness of the NCEPR dataset make it attractive for climate studies on topics ranging from climate variability and synoptic climatological analyses to comparative analyses of GCM performance [31]. NCEP data was used to compare the results obtained from the models during the historical simulation period. NCEP has a resolution of 2.5° latitude and 2.5° longitude.

ii. Third Version Coupled Global Climate Model (CGCM3): This is the third version of the Canadian Coupled Global Climate Model (CGCM3.1) and is a widely used model for statistical downscaling input. Details of the model are described by McFarlane et al., 2005 [32]. Additional information can also be obtained from (http://www.ec.gc.ca/ccmac-cccma/default.asp?lang=En&n=89039701-1. The CGCM3 has a resolution of 3.75° latitude and 3.75° longitude.

iii. Second Generation of Earth System Model (CanESM2): Developed at the Canadian Centre for Climate Modelling and Analysis (CCCma), this model consists of the physical coupled

atmosphere–ocean model CanCM4 coupled to a terrestrial carbon model (CTEM) and an ocean carbon model (CMOC) [33]. CanESM2 provided CCCma's long-term climate simulations for Phase 5 of the Coupled Model Inter-comparison Project, which in turn informed the Fifth Assessment Report (AR5) of the Intergovernmental Panel on Climate Change [34]. The CanESM2 model has a resolution of 2.79° latitude and 2.81° longitude.

These models were used both for the Special Report on Emissions Scenarios and the Representative Concentration Pathway (RCP) Scenarios. The SRES Scenarios were also included with the RCP Scenarios and the results compared with the previous studies undertaken in the region. The SRES (Special Report on Emissions Scenarios) Scenarios were those used by the IPCC until the Fourth Assessment Report, and these four narratives (A1, A2, B1, and B2) cover different demographic and technological futures. Specifically, they address a fossil-fuel-intensive future (A1F1 scenario) versus a predominantly non-fossil-fuel future (A1T).

For new scenarios of the Fifth Assessment Report of the IPCC, the Representative Concentration Pathways (RCPs) were developed. Each pathway represents a set of internally consistent socioeconomic assumptions that result in four levels of radiative forcing: RCP8.5, RCP6, RCP4.5, and RCP2.6. The Concentration Pathways are four greenhouse gas concentration (not emissions) trajectories adopted by the IPCC for its Fifth Assessment Report (AR5) in 2014. It supersedes the Special Report on Emissions Scenarios (SRES) projections. So far, four RCP scenarios exist and each assumes a different level of radiative forcing by the year 2100: 3, 4.5, 6 and 8.5 W/m^2 [35]. The RCP Scenarios considered in this study fall under RCP4.5 and RCP8.5. RCPs describe a wide range of potential issues concerning climate change like greenhouse gases, air pollutants, emissions, and land use. RCPs have broken new grounds in several ways. They include some of the highest and lowest scenarios of greenhouse gases that have been recently examined by the climate research community.

2.3. Downscaling Method

Climate scenarios from a global climate model (GCM) are usually at a large scale and, for that reason, they are not suitable for impact and adaptation studies that require detailed local data. The regional outputs from a GCM are therefore "downscaled" using one of two methods—dynamical downscaling or statistical downscaling.

Statistical downscaling has standard and accepted statistical procedures.It is computationally inexpensive, able to directly incorporate the observational record of the region, etc. A number of studies indicate that the SDSM yields reliable estimates of extreme temperatures, seasonal precipitation totals, and areal and inter-site precipitation behavior [3,10,20,36]. The SDSM calculates statistical relationships based on multiple linear regression techniques between large-scale (the predictors) and local climate variables (the predictand) [37].

The SDSM software manages tasks like data quality control and transformation, screening variables, model calibration, frequency analyses, statistical analysis, scenario generation, and graphing of climate data. All the data are processed using the SDSM software. The mathematical details of this model are provided in the study by Wilby et al. [38]. As the values are normally distributed, transformation was not undertaken on temperature results in the software [18]. However, for the daily rainfall, the fourth root transformation was used as the data were skewed and as its model was conditional. Transforming created a more normal distribution in the precipitation data.

The SDSM model contains two separate sub-models to determine the occurrence and amount of conditional meteorological variables (or discrete variables), such as precipitation, and the amount of unconditional variables (or continuous variables), such as temperature or evaporation. Therefore, the SDSM can be classified as a conditional weather generator in which regression equations are used to estimate the parameters of daily precipitation occurrence and amount separately, making it slightly more sophisticated than a straightforward regression model. The SDSM yields reliable estimates of extreme temperatures, seasonal precipitation totals, and areal and inter-site precipitation behavior. This freely available software enables the production of climate change time series at sites for which

there are sufficient daily data for model calibration, as well as archived General Circulation Model (GCM) output to generate scenarios for the 21st century. The SDSM can also be used as a stochastic weather generator or to fill in gaps in meteorological data [10].

The model structure in the SDSM is given in Figure 2.

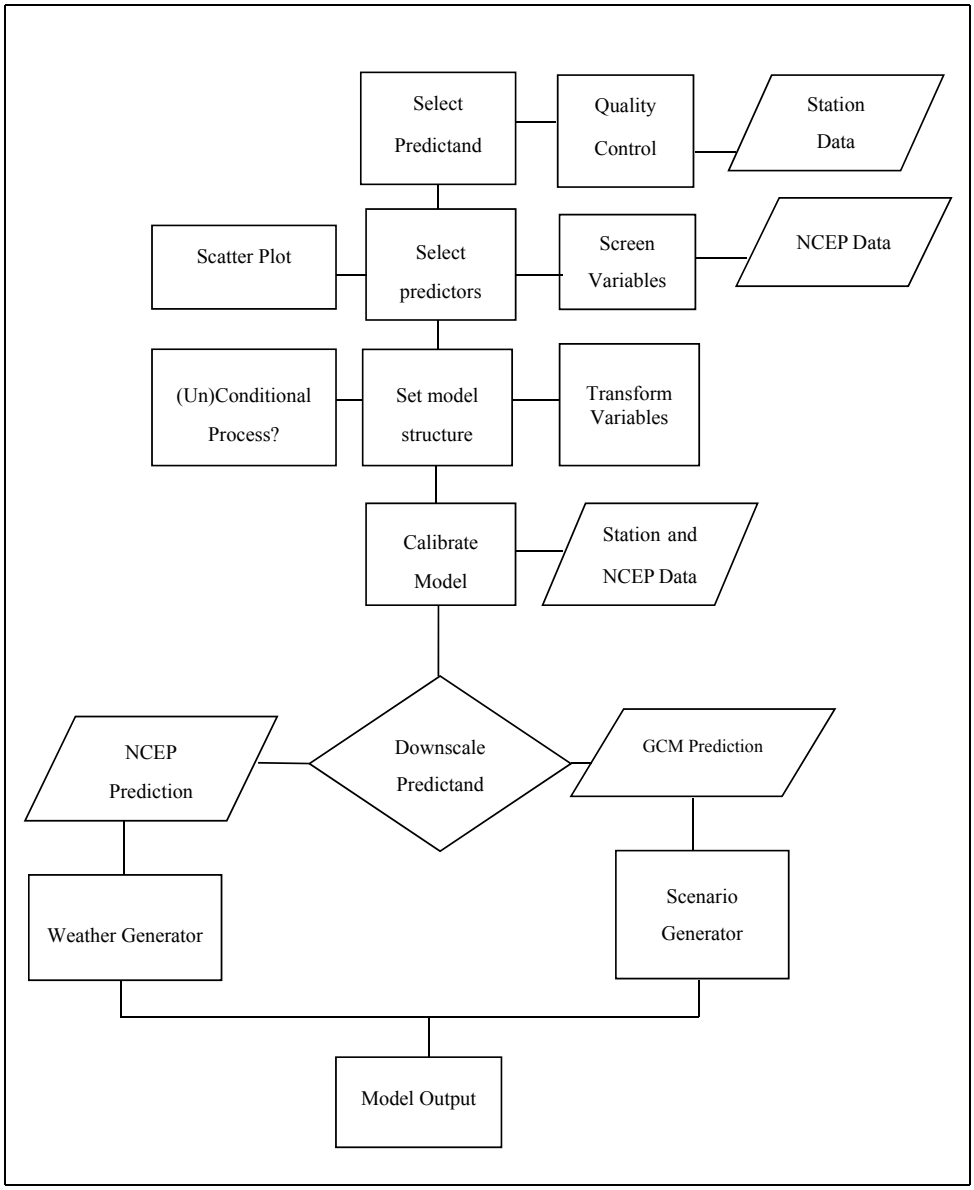

Figure 2. SDSM Version 4.2 climate scenario generation, adapted from [39].

2.4. Selection of Predictors

Selecting a predictor is an important step in the downscaling process. It is an iterative procedure consisting of a rough screening of the possible settings and predictors, which is repeated until an objective function is optimized [38]. The variables with the highest correlation are selected using the screen variable tool in the SDSM. First, all the predictors from historical records are correlated with the past observed maximum temperature, minimum temperature, and precipitation in the past. Then the predictors with the highest correlation are selected. The selected number of predictors varies from three to five. The correlation statistics and *p*-values are used to explain the strength of the relationship between the predictor and predictand. The highest correlation values represent a higher

degree of association and smaller p-values describe a better chance for an association between variables. The most appropriate sets of predictor variables are selected on the basis of partial correlation and percentage of explained variance (E) analysis among the predictand and the individual predictors. In order to have better prediction results, all the correlations with a *p*-value less than 0.05 were selected.

The default bias correction factor in the SDSM is 1 for temperature. The 'Bias Correction' parameter compensates for any tendency in the downscaling model to over- or under-inflate the variance of the conditional process. The selected variables, screened for precipitation and temperature at Entoto station and Addis Ababa Observatory, are given in Table 1.

Table 1. Selected predictor variables from the General Circulation Models.

Predictors	Code	Addis Ababa Station			Entoto Station		
		Max. Temp	Min. Temp	Precip.	Max. Temp	Min. Temp	Precip.
Surface zonal velocity	p_u	✓					✓
500 hPa airflow strength	p5_f			✓	✓		
500 hpa geopotential height	p500	✓	✓		✓		
Surface meridional velocity	P_v	✓			✓		
500 hPa zonal velocity	p8_v		✓			✓	✓
Surface specific humidity	shum			✓			✓
Mean temperature at 2 m	temp	✓	✓				
500 hPa zonal velocity	p5_u				✓		
Surface vorticity	p_z	✓			✓		
850 hpa divergence	p8zh						✓
850 hPa airflow strength	p8_f			✓			
850 hpa zonal velocity	p8_u					✓	
850 hPa meridional velocity	p8_v						✓
850 hpa vorticity	p8_z.		✓		✓	✓	
500 hPa divergence	p5zh		✓			✓	
Surface wind direction	p_th:			✓			
Surface airflow strength	p_f			✓			

2.5. Model Calibration, Validation, and Extreme Event Indices Selection

In other words, to calibrate the SDSM, regression models for every month of the year are constructed with the relationship between predictand and selected predictors. The first 15 years of the station (predictand) and reanalysis (predictors) datasets are used for calibration, and the last 15 years for evaluation of the calibration. The period 1989–1998 was used for model calibration and 1999–2003 for model validation for Entoto station. The difference in time span for the calibration and validation periods for Addis Ababa and Entoto stations is due to data availability. When calibrating a model the coefficient of determination (R^2) and Standard Error (SE) factors are considered. The calibration algorithm reports the percentage of explained variance and standard error for each regression model type (monthly, seasonal, or annual averages). These data should inform assessments of the significance of climate changes projected by the statistical downscaling.

One of the main concerns while assessing extreme climate events is properly defining extreme indices for climate variables (temperature and precipitation). Different studies have defined varying indices according to their study regions' climates. While these indices may have similar names, their definitions may vary. Recently, the Expert Team on Climate Change Detection Indices (ETCCDI) has developed a core set of 27 indices to analyze the wide range of extreme climate changes. For this study, six temperature indices and six precipitation indices out of the 27 ETCCDI' recommendations were selected to explore possible changes in temperature extremes in the future in Addis Ababa. In addition to the definitions given by the ETCCD for the extreme events, an additional definition given by Donat et al. [40] was used. Extreme events such as heat waves and heavy rains result in severe climate-related damage and hence emphasis is given to analyzing the changes in extreme events under a changing climate. The temperature and precipitation indices used in this study are summarized in Table 2.

Table 2. Extreme indices of temperature and precipitation.

Temperature Indices			
Code	*Description*	*Indices definition*	*Units*
TXx	Hottest days	Maximum values of daily maximum temperature	°C
TNx	Hottest nights	Maximum values daily minimum temperature	°C
TXn	Coldest days	Minimum values of daily maximum temperature	°C
TNn	Coldest nights	Minimum values of daily minimum temperature	°C
TX_90P	Hot Days	(90th percentile value of data describes that at least 90% of the values in the data are less than or equal to this value) [41]	°C
TN_90P	Hot Nights	90th percentile value of data describes that at least 90% of the values in the data are less than or equal to this value % [41]	
Precipitation Indices			
Rx1day	Max 1-day precip.	Monthly maximum 1-day precip.	mm
Rx5day	Max 5-day precip.	Monthly maximum consecutive 5-day precip.	mm
99%le	Extremely wet days	Annual total precip. from days >99th percentile	mm
PRCPTOT	Annual total wet day precip.	Annual total precip. from days ≥1 mm	mm
CDD	Consecutive dry days	Maximum number of consecutive dayswhen precipitation <1 mm	days
CWD	Consecutive wet days	Maximum number of consecutive dayswhen precipitation ≥1 mm	days

2.6. Quantile Mapping and Delta Statistics

Quantile Mapping (QM) is an emerging downscaling approach that is utilized to remove bias from observed and simulated rainfall using cumulative distribution functions. It estimates quantiles for both datasets, then forms a transfer function by interpolation between corresponding quantile values. The number of quantiles is a free parameter. A quantile–quantile plot is a basic graphical approach for checking normality by comparing sample quantiles against population quantiles. Thus, quantile–quantile downscaling consists of a probability plot of model outputs against observed values, with both corresponding to the same probability [42] or using empirical distribution functions [43]. It assumes that, although the two time series are independent, they describe the same variable at approximately the same location and, therefore, must have unique probability density functions (PDFs).

The delta method is a simple, yet widely used method [31] to create scenario time series from GCM output. The method uses the delta method of the SDSM for future projections and changes in extreme indices. The standard approach for the delta method is that the GCM-simulated difference for each calendar month (absolute difference for temperature and relative difference for precipitation) between a future period and the baseline period is determined and then this is superimposed on the historical daily temperature and precipitation series [44].

In the SDSM, a change in precipitation is obtained by:

$$\Delta 2020\text{s} = \frac{(v2020s - vbase) \times 100}{vbase}. \quad (1)$$

The same is true for changes in 2050 and 2080.

For the absolute value calculation (temperature in this case)

$$\Delta 2020 = v2020 - vbase \quad (2)$$

The value at 2050 and 2080 is also obtained by the same formula explained in Equation (2).

Vbase is the mean of all ensembles (or a specific ensemble if selected) for each statistic for the baseline period. Likewise, *V*2020s is the mean of all ensembles (or a specific ensemble) for each statistic for period A, and so on for *V*2050s and *V*2080s [39].

3. Results and Discussion

3.1. Performance of the SDSM Model Validation and Calibration Result

Prior to future scenario construction the results of the observed data of maximum temperature, minimum temperature and precipitation are correlated with the modeled data during the calibration

and validation periods using the coefficients of determination and standard errors. The calibration period for Addis Ababa station is 1971–1985 and for Entoto station it is 1989–1998. The coefficient of determination for Addis Ababa Observatory is 0.63 (NCEP and CanESM2) and 0.4 (CGCM3) for maximum temperature and 0.68 (NCEP) and 0.66 (CanESM2 and CGCM3) for minimum temperature during the calibration period for both CanESM2 and CGCM3 models. The correlation coefficient of determination for precipitation is 0.09, 0.011, and 0.010 in the NCEP, CanESM2, and CGCM3A2 models, respectively, for Addis Ababa station. In the unconditional process the calibration and validation period's coefficient of determination (R^2) and standard error are similar. The R^2 for precipitation at Addis Ababa station is higher than in the validation period. The R^2 for precipitation is the lowest due to it being a conditional process and having a less regular distribution than the temperature distribution. Unconditional models assume a direct link between the regional-scale predictors and the local predictand. For example, local wind speeds may be a function of gridded airflow indices such as the zonal or meridional velocity components. Conditional models, such as for daily precipitation amounts, depend on an intermediate variable such as the probability of wet-day occurrence [36]. The R^2 and standard error of the calibration and validation period are summarized in Table 3.

Table 3. Result of model calibration and validation.

Addis Ababa obs. Calibration Period (1971–1985)				Addis Ababa obs. Validation Period (1986–2000)		
Model	**Maximum Temperature**	**Minimum Temp**	**Precipitation**	**Maximum Temperature**	**Minimum Temp**	**Precipitation**
	R^2	R^2	R^2	R^2	R^2	R^2
	SE	SE	SE	SE	SE	SE
NCEP	0.63	0.68	0.09	0.58	0.63	0.02
	1.34	1.21	9.02	1.45	1.12	9.55
CanESM2	0.63	0.66	0.011	0.57	0.65	0.01
	1.36	1.18	9.00	1.46	1.17	9.50
CGCM3	0.64	0.66	0.01	0.58	0.64	0.06
	1.34	1.17	9.00	1.44	1.17	9.58
Entoto Station Calibration Period (1989–1998)				Entoto Station Validation Period (1999–2003)		
NCEP	0.58	0.65	0.031	0.60	0.40	0.01
	1.32	1.10	9.30	1.4	1.00	8.20
CanESM2	0.62	0.64	0.043	0.63	0.41	0.04
	1.35	0.09	9.30	1.36	0.97	8.20
CGCM3	0.61	0.65	0.030	0.62	0.43	0.04
	1.36	1.10	9.37	1.38	1.00	8.22

R^2: Coefficient of determination; SE: Standard Error. Autoregressive terms are added on all R^2 and SE values in SDSM.

The performance of the model is tested by constructing the plots for the observed and modeled data during the calibration period. The calibration period for Addis Ababa station is 1986–2000 and the calibration period for Entoto station is 1999–2005. As observed from the graphs, the observed maximum temperature values and the graphs are well simulated with pattern characteristics both at Addis Ababa and Entoto stations. Except for the CGCM3 at Addis Ababa station, all the models overestimate the minimum temperature for values below 8 °C and above 11 °C. Details of the models of the quantile plots are shown in Figure 3.

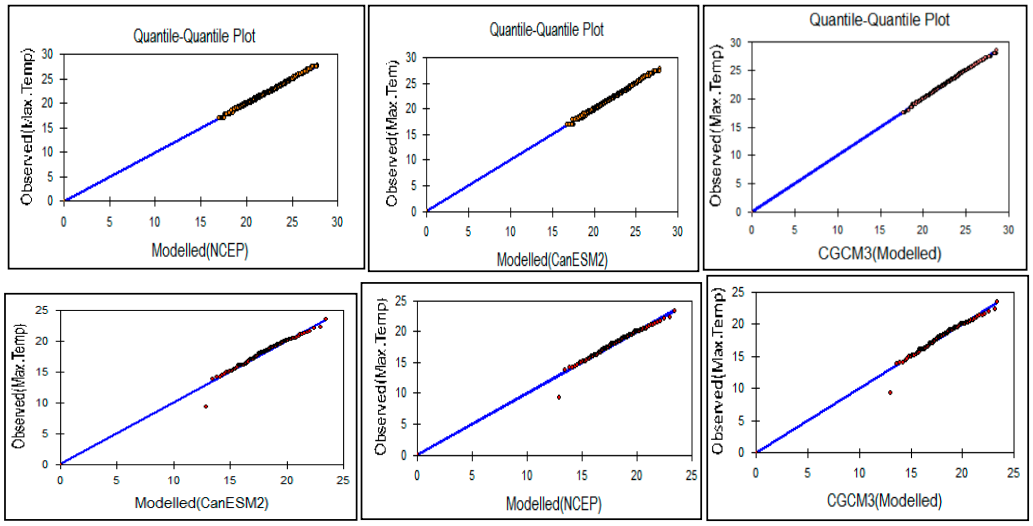

Figure 3. Quantile–quantile (Q–Q) plots of observed versus modeled maximum temperature (°C) at Addis Ababa (upper) and Entoto (bottom) stations.

The plot is a normally distributed population. The modeled maximum temperatures are exactly the same as the observed temperatures, shown as fitted lines for the Q–Q plots (except for records for values less than 12 °C that overestimate the maximum temperature at Entoto station). The Q–Q plot for minimum temperature is normally distributed at Addis Ababa station. At Entoto station, however, all models overestimate the highest and lowest values, i.e., below 6 °C and above 10 °C. The Q–Q plot fits between 6 °C and 10 °C. The Q–Q plots of minimum temperature at Addis Ababa and Entoto stations are given in Figure 4.

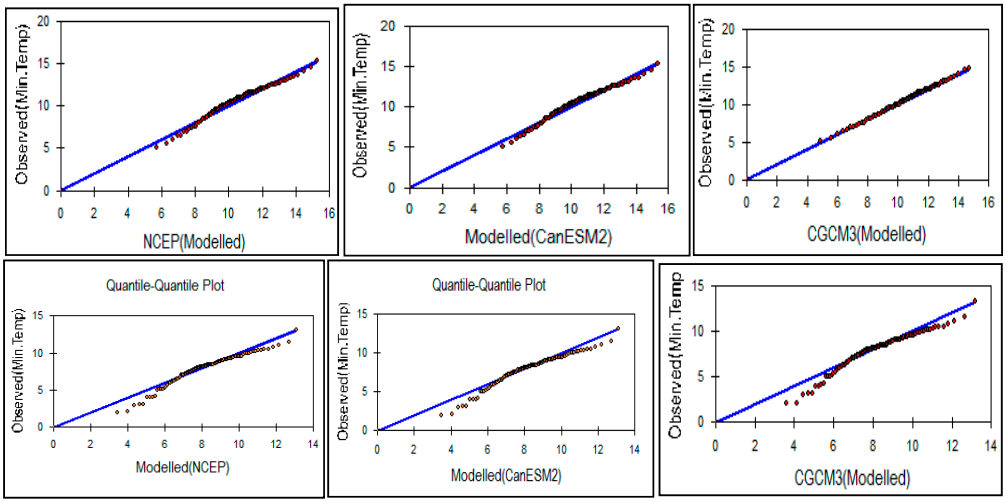

Figure 4. Quantile–quantile plots of observed versus modeled minimum temperature (°C) at Addis Ababa (upper) and Entoto (bottom) stations during the validation period.

Similarly, simulated daily precipitation is modeled against the observed precipitation. All the model results indicate that there is overestimation for results that are greater than 20 mm and underestimation for results that are greater than 20 mm. The Q–Q plots of daily precipitation of the validation period are given in Figure 5.

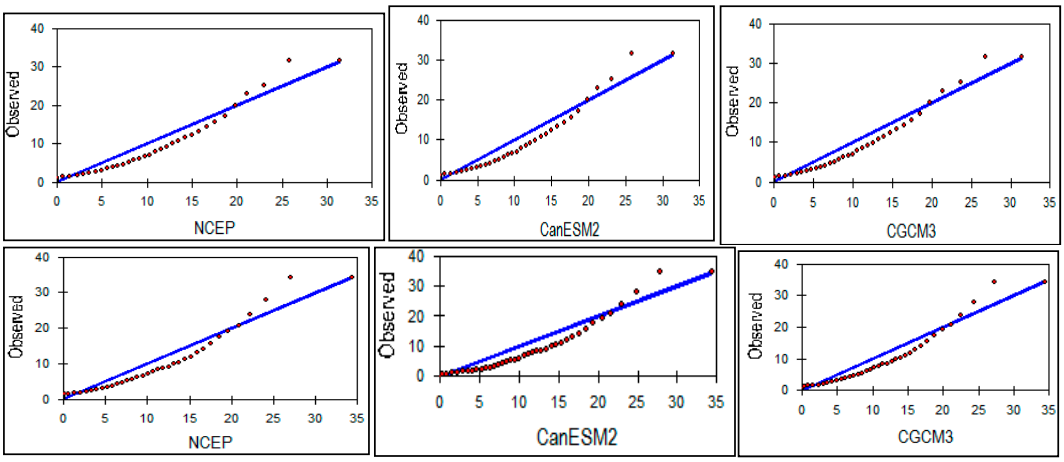

Figure 5. Observed and modeled precipitation at Addis Ababa (upper) and Entoto (bottom) stations during the validation period.

3.2. Future Temperature and Precipitation Change Scenarios

3.2.1. Temperature

Future temperature predictions from all downscaled models under different scenarios show that both maximum and minimum temperature increase in magnitude and intensity in Addis Ababa up to the end of this century. According to the models, the change ranges from 0.03 °C for the minimum temperature at Entoto in 2020 to 2.1 °C by 2080 using the CGCM3A2 projections and considering RCP4.5 in the worst case scenario for maximum temperature. All models project increases of the maximum temperatures from 0.03 °C–0.21 °C using the CGCM3A2 and RCP4.5 models in 2020. In 2050, the maximum temperature increases by 1 °C in the CGCM3A2 scenario. In all scenarios the projected maximum temperature in 2020 is the highest at Entoto station. The minimum temperature is also projected to increase by 1.03 °C in 2080 under the A1B scenario at Entoto station. The minimum temperature change at Addis Ababa station is the lowest in 2020. The minimum temperature at Entoto station increases more than the maximum temperature in the 2020s. In 2050 the minimum temperature ranges from 0.29 °C (RCP4.5) to 0.32 °C (RCP8.5) at Addis Ababa station. In 2080, the CGCM3A2 model projects an increase of 0.6 °C for the minimum temperature at Entoto station and 0.75 °C under the RCP8.5 model at Addis Ababa station. It is observed that the rate of change for the minimum temperature at a higher altitude is much higher than the rate of change at a lower altitude at Addis Ababa. However, the change in maximum temperature is higher in the downtown than in the peripheral areas (Entoto).

The results from all models under multiple scenarios indicate that precipitation will continue increasing until the end of this century. In the CanESM2 model under the RCP8.5 scenario and the CGCM3A2 model, the precipitation is projected to increase by 16.6% compared to the baseline period. Though the changes in the precipitation value by 2020 are not significant, as concluded from the results of future scenarios, the prediction of precipitation will continue to increase in 2050 and 2080. In 2050, under the worst-case scenario, precipitation will increase by 8.7% compared to the baseline period. In 2080, the highest projection is 16.6% (RCP8.5), followed by the CGCMA2 scenario, which is 11.7% at Addis Ababa station. At Entoto station, the rate of change in 2080 is projected to be 2.58%, 8%, 7.8%, and 11.8% under the RCP4.5, RCP8.5, CGCM3A1B, and CGCM3A2 scenarios, respectively.

The summaries of maximum and minimum temperature predictions from three models for the six scenarios are presented in Table 4.

Table 4. Downscaled temperature (°C) and precipitation (%) scenarios (changes).

Station	Predictands	Year	CanESM2		CGCM3	
			RCP4.5	RCP8.5	A1B	A2
Addis Ababa obs. (Baseline period 1971–2000)	Maximum Temperature	2020s	0.09	0.06	0.09	0.12
		2050s	0.41	0.61	0.77	1.00
		2080s	0.52	1.20	1.31	2.06
	Minimum Temperature	2020s	0.02	0.02	0. 36	0.07
		2050s	0.239	0.39	0.18	0.14
		2080s	0.30	0. 70	0.28	0.27
	Precipitation (% Difference)	2020s	1.28	1.30	1.08	2.30
		2050s	3.82	6.20	4.02	8.70
		2080s	7.49	16.6	7.40	11.7
Entoto (Baseline period 1989–2003)	Maximum Temperature	2020s	0.09	0.09	0.17	0.21
		2050s	0.22	0.41	0.57	0.56
		2080s	0.28	0.71	0.84	1.01
	Minimum Temperature	2020s	0.03	0.03	0.25	0.20
		2050s	0.07	0.09	0.69	0.57
		2080s	0.10	0.14	1.04	0.99
	Precipitation (% Difference)	2020s	1.10	0.60	1.24	1.36
		2050s	2.57	4.80	2.80	2.70
		2080s	2.58	8.00	7.80	11.8

3.2.2. Changes in Temperature Extreme Indices

The results of the extreme events analyses are important for this study. Temperature indices are studied based on their changes within each season. In all the seasons, the maximum value of the maximum temperature (TXx) is projected to increase in 2080 with the highest projection reaching 3.20 °C (A2). Except for the RCP8.5 scenario, the CGCM3A2 scenario in 2020 and CanESM2 RCP8.5 scenario in 2050 all the maximum value of the minimum temperatures (TNx) will increase to a non-significant degree. In winter and spring the TNx value decreases, while in summer and autumn the TNx value is projected to increase. The year-round prediction has a positive value. Regarding the minimum values of the minimum temperature (TNn), half of the scenarios indicate that TNn decreases. In 2050 and in 2080 all the CanESM2 scenarios project that the TNn value decreases.

TX_90P and TN_90P are expected to increase in 2020, 2050, and 2080. In autumn the models predicts the lowest TN_90P, and in spring the TX_90P is predicted to have positive values. The highest value of TX_90P is 3.18 °C in autumn of 2080 under RCP8.5, followed by 3.07 °C in spring. Similarly, TN_90P (°C) is the highest in summer for 2080 (RCP8.5), reaching 1.3 °C. All models predict that the TN_90P value will increase by less than 1 °C. It is only in the RCP 8.5 scenario for the summer of 2080 that the projection reaches as high as 1.37 °C. Details of the temperature indices based on the seasonal changes in 2020, 2050, and 2080 are given in Figure 6.

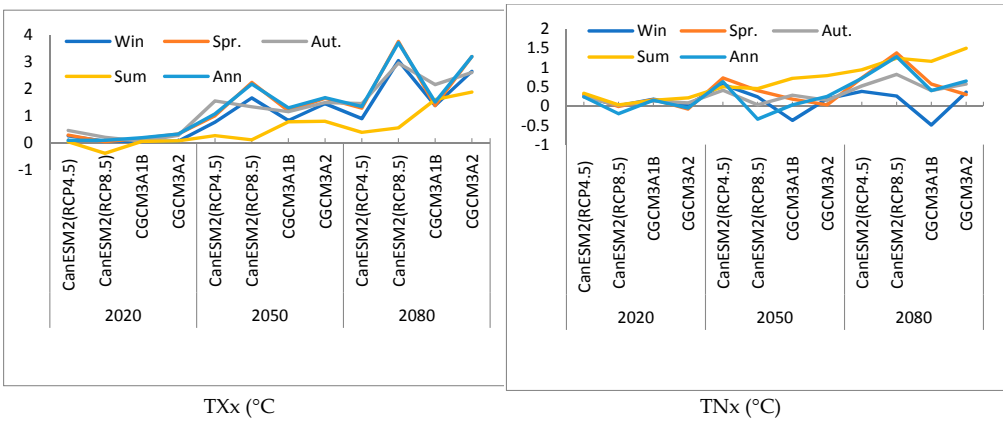

TXx (°C TNx (°C)

Figure 6. *Cont.*

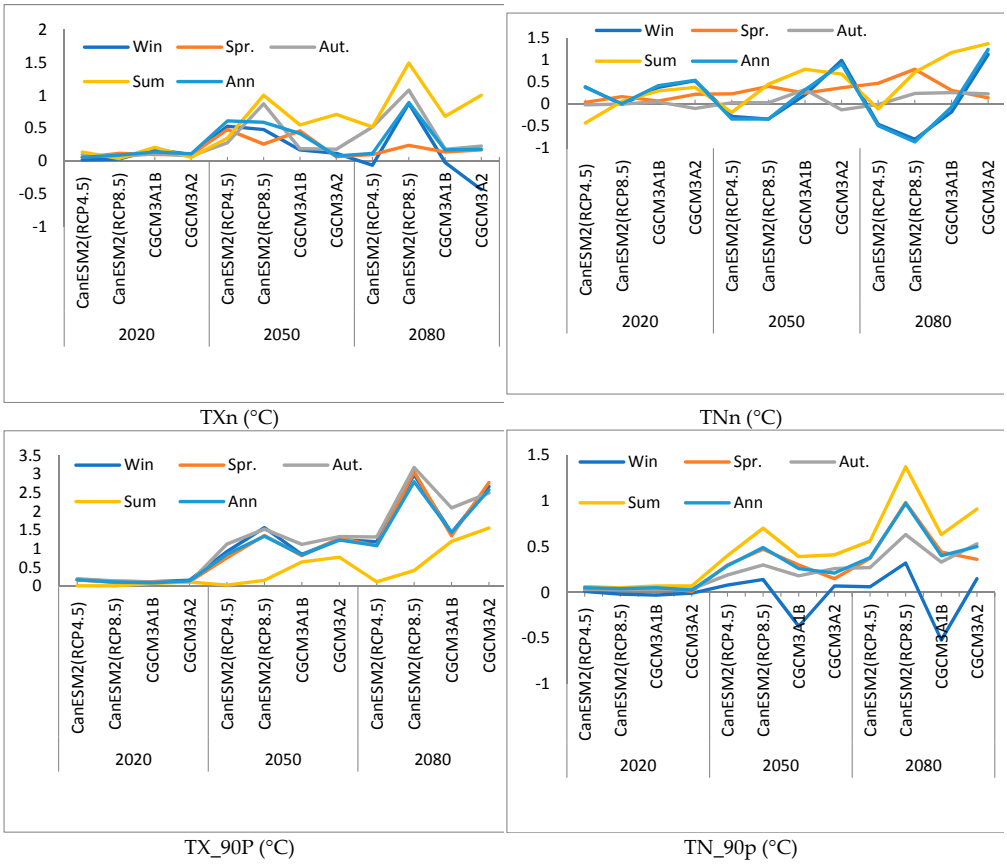

Figure 6. Changes in selected temperature extreme indices.

3.2.3. Future Changes in Precipitation Extreme Indices

The precipitation indices show different changes in intensity and amount, indicating incremental changes in the precipitation amount. Except for the RCP8.5 scenarios in 2020, CGCM3 in 2050, and A2 in 2080, all the models predict Rx1 increases. The highest value is 7.22% in 2050. However, specifically for autumn, the prediction falls to −11.3%. Similarly, the Rx5day is expected to increase in 2050 for most of the models. The highest Rx5day predictions are 21% (RCP4.5) and 17.6% (RCP8.5) in winter 2020 and 2080, respectively. Regarding the total precipitation index (PTOT), the highest is in 2080 at 17.96% (RCP8.5). The greatest change is in the winters of the 2080s, for which a value of 29.30% (RCP4.5) is predicted, and in summer a value of 20.9% (RCP8.9) and 19.13% (CGCM3A2). Consecutive wet days are expected to increase by 27.3% (RCP8.5) in 2050, and the highest value for this is in summer 2080 at 28% (RCP8.5). Consecutive dry days are projected to decrease from 2020–2080 in all models, with ranges from −0.6% in 2020 to −19.8% in 2080. Details of the precipitation indices are presented in Figure 7. The results indicated positive trends for the maximum value of the maximum temperature (TXx), warm days (TX90P), and warm nights (TN90P).

Figure 7. Selected precipitation indices in percentages.

4. Discussion

This study investigated changes in future maximum temperature, minimum temperature, precipitation, and their extremes in Addis Ababa, through downscaling from selected general circulation models. The considered changes were analyzed up to the end of the 21st century, taking observed station data from two meteorological sites from 1971–2003 as the baseline. The aim of the downscaling was to predict site-specific future temperature and precipitation extreme changes, in order to assess possible future risks from climate change. The results indicate that temperature and its extremes are expected to increase in the city, with the highest rate occurring in the 2080s. The trends, changes, highest moderate and extreme changes in both climatic elements and extreme events have

been identified. For all three future periods and under all scenarios, almost all intensity extreme indices showed incremental increases. We conclude that more warming is expected towards the end of this century.

It should not be surprising that this study's findings are in line with many downscaling works undertaken in Ethiopia, particularly on temperature results, though the previous studies were not conducted on an urban scale. Climate model projections of climate in Ethiopia show warming in all four seasons across the country but a wide range of rainfall patterns, with no clear direction of change. Table 5 describes the summary of many downscaling studies in Ethiopia, using statistical models.

Table 5. Comparison of obtained changes with statistically downscaled research in different parts of Ethiopia.

Model	Study Area	Temperature	Precipitation	References
ECHAM 5 and HADCM3	Across Ethiopia and Kenya	Clear trends at all locations towards warmer conditions in the future.	ECHAM5 model shows a trend towards wetter annual conditions over most parts.	[23]
HadCM3 A2a and B2a and CanESM2 (RCP2.6, 4.5 and 8.5)	Upper Blue Nile River Basin	Maximum temperature rise by 0.4 °C to 2.9 °C and minimum temperature rise by 0.3 °C to 1.6 °C.	Relative changes in mean annual precipitation ranges from 2.1–43.8%.	[45]
HadCM3 A2 and B2	Lake Hawasa	Maximum temperature increase by 1.6–1.8 °C and minimum temperature by 1.54–1.7 °C in 2050.	Trends in annual rainfall do not show statistically meaningful trends between years.	[46]
CGCM3.1 and REMO	Baro-Akobo Basin	Maximum temperature rises by 1.3 °C (REMO A1B and B1) and 2.55 °C (CGCM3.1).	24% (REMO) and 23% (CGCM3.1) rise in 2050.	[47]
HadCM3 A2a	Northwestern Ethiopia	The increase in mean maximum and minimum temperature ranges from 1.55–6.07 °C and from 0.11–2.81 °C, respectively, in the 2080s.	Decrease in amount of annual rainfall and number of rainy days in 2080s.	[18]
HadCM3-A2	Upper Blue Nile Basin	The minimum and maximum temperature will increase by 3.6 °C and 2.4 °C, respectively, towards the end of the 21st century.	Dry season rainfall amounts are likely to increase and wet season rainfall to decrease.	[48]

From the results obtained from this study and other general studies in Ethiopia, it should be noted that the increases in temperature and rainfall are real. Despite climate change being a major global issue today, in Addis Ababa it does not garner considerable attention. All current government plans are focused on supplying the ordinary needs of residents; the climate issue seems to be mostly neglected. The city is busily supplying basic infrastructural and social demands because of high population growth, which of course plays a pivotal role in modifying the local climate of the city. Within this framework, the awareness of future downscaled climatic data for environmental planning is generally limited.

However, considering future changes and prioritizing their incorporation into plans for the city is inevitable for several reasons. First, there is an elevation difference of 1000 m within the city. Due to this, all places might not be affected equally by climate change, and hence prioritization for an intervention mechanism is important. Second, there is a high rate of population growth. Studies reveal that the projected population of Addis Ababa city, with a high population growth rate (3.3%), is about 7 million by the year 2039, which would exacerbate water problems in the city [49]. Thirdly, there is a high rate of urbanization. Urban heat islands could exacerbate the climate problem as the studies indicate the downtown areas are getting hot, and the land surface temperature is increasing over time. The urban areas are expanding at the expense of forests and agricultural land [50–52].

5. Conclusions

This study attempts to analyze historic climate change trends and extremes, and constructs future temperature and precipitation scenarios up to the end of this century, in 30-year intervals, based on

daily predictor data from two stations in Addis Ababa city. The analyses also consider future extreme events by analyzing six temperature indices and six precipitation indices that could prevail in Addis Ababa city based on the definitions set by the ETCCD to study climate change extremes. Two GCMS have been statistically downscaled under four scenarios (two SRES and two RCP). The predictors of the model were screened and selected based on the R^2 and *p*-values. The study found a good correlation between the modeled and observed results during the validation period. It also compares the results of the modeled data against the observed values for the base periods of 1971–2000 for Addis Ababa station and 1989–2005 for Entoto station.

All the models perform well in predicting the mean values during the validation period. Their good performance is displayed in quantile–quantile plots and PDFdf curves. Future scenarios predict that both the maximum and minimum temperature will increase up to the end of the century. All the models predict the change will be highest after 2020. The changes in climatic elements up to 2020 are not significant. However, in 2050, and 2080, the predictions are higher. The changes in maximum temperature reach 2.06 °C (CGCM3A2) in the worst-case scenarios in 2080. Similarly, the increase in the minimum temperature reaches 1.03 °C in 2080 (CGCM3A1B). Except for the coldest nights (TNn), the mean temperature and other temperature indices are projected to increase up to the end of the century. Precipitation will also increase by 11.8% (CGCM3A2) or 16.6.2% (CanESM2 RCP8.5) by 2080. All the models also predict an increase in precipitation. The changes in precipitation are seasonally varied. The total precipitation increases by 29% (RCP4.5) in winter and 20.9% (RCP8.5) in summer by 2080 in the worst-case scenarios. Maximum one-day and five-day precipitation will also significantly increase in winter and summer in 2080. All the indices of precipitation will additionally increase to the end of the century compared to the baseline period, except for consecutive dry days (CDD).

Although there is a seasonal difference in the amount and changes in extreme events, there is good agreement among the models under different scenarios regarding the increase of precipitation and temperature. All the values of the models indicate similar projections; however, the magnitude of the prediction varies from one model to another. Except for the minimum temperature at Addis Ababa Observatory in the SRES scenarios of the CGCM3A2 model, temperature values are highly overestimated (even more than in RCP8.5) at both Entoto and Addis Ababa stations. Regarding precipitation, in 2020 and 2050 the precipitation value is overestimated by the SRES in CGCM3A2; however, after 2050, the RCP8.5 better models the precipitation than SRES, except at Entoto station. The analysis also shows that there is no significant negative trend in temperature and precipitation despite the variability in amounts.

Generally, the city will experience an increase in temperature, which will gradually modify the existing temperature conditions, resulting from high urban activity and climate change.

As a result, the effect of elevation differences, which ranges by 1000 m, will be less in every direction of the city. The city has been affected by flood-induced damage due to the low level of infrastructure development and the poor quality of housing. Moreover, with the expected rise of precipitation due to global climate change, the city will continue to experience flooding vulnerability. Hence, it is recommended that city planning integrates the findings of this research to develop better adaptation mechanisms. Further studies also need to be undertaken by adding various model ensembles in order to avoid prediction inconsistency.

Author Contributions: G.F. conceived and designed the experiments, set up the model and tuning, conducted the analysis and is responsible for writing; G.Z. and W.B. helped developing the idea, supervised the analyses, review the results and the writing process; E.G. contributed to improving the methodology and provided critical discussions.

Funding: This work is supported by Addis Ababa University Thematic Area Research Fund; fund number TR/11/2013.

Acknowledgments: The authors would like to thank the German Academic Exchange Service (DAAD) for providing an in-country scholarship to the corresponding author for his PhD study at Addis Ababa University, Ethiopian Institute of Architecture, Building Constriction and Urban Development. The authors would also like to thank the Potsdam Institute for Climate Impact Research for allowing a corresponding author a six-month

research visit in Potsdam, Germany. The authors would further like to thank the Meteorological Service Agency of Ethiopia for providing us with meteorological data.

Conflicts of Interest: The authors declare that they have no conflicts of interest.

References

1. Intergovernmental Panel on Climate Change. Climate Change 2014: Impacts, Adaptation, and Vulnerability WGII. AR5 Summary for Policymakers. 2014. Available online: http://www.ipcc.ch/report/ar5/wg2/ (accessed on 15 September 2016).
2. Intergovernmental Panel on Climate Change. Summary for Policy Makers. Fact Sheet Climate Change in Africa—What Is at Stake? Excerpts from IPCC Reports, the Convention, & BAP Compiled by AMCEN Secretariat. 2007. Available online: https://www.ipcc.ch/pdf/assessment-report/ar4/wg2/ar4_wg2_full_report.pdf (accessed on 15 September 2016).
3. Abbasnia, M.; Toros, H. Future changes in maximum temperature using the statistical downscaling model (SDSM) at selected stations of Iran. *Model. Earth Syst. Environ.* **2016**, *2*, 1–7. [CrossRef]
4. Cheng, L.J.; Zhu, J. 2017 was the warmest year on record for the global ocean. *Adv. Atmos. Sci.* **2018**, *34*, 261–263. [CrossRef]
5. Srivastava, A. Vulnerability to Climate Change & Variability: An Investigation into Macro & Micro Level Assessments—A Case Study of Agriculture Sector in Himachal Pradesh, India; Report on the Patterns of Disaster Risk Reduction Actions at Local Level. 2015. Available online: http://www.unisdr.org/campaign/resilientcities/assets/documents/privatepages/VULNERABILITY%20TO%20CLIMATE%20CHANGE%20&%20VARIABILITY.pdf (accessed on 23 November 2017).
6. Hassaan, M.A.; Abdrabo, M.A.; Masabarakiza, P. GIS-based model for mapping malaria risk under climate change case study: Burundi. *J. Geosci. Env. Protec.* **2017**, *5*, 102–117. [CrossRef]
7. Mwangi, K.M.; Mutua, F. Modeling Kenya's vulnerability to climate change—A multifactor approach. *Int. J. Sci. Res.* **2015**, *4*, 12–19.
8. Conway, D.; Schipper, L.E.F. Adaptation to climate change in Ethiopia: Opportunities identified from Ethiopia. *Glob. Environ. Chan.* **2011**, *21*, 227–237. [CrossRef]
9. McSweeney, C.; New, M.; Lizcano, G. *UNDP Climate Change Country Profiles: Ethiopia*; United Nations Development Programme: New York, NY, USA, 2010.
10. Wilby, R.L.; Dawson, C.W. The statistical downscaling model (SDSM): Insights from one decade of application. *Int. J. Clim.* **2013**, *33*, 1707–1719. [CrossRef]
11. Omondi, P.A.; Awange, J.L.; Forootan, E.; Ogallo, L.A.; Barakiza, R.; Girmaw, G.B.; Fesseha, I.; Kululetera, V.; Kilembe, C.; Mbati, M.M.; et al. Change in temperature and precipitation extremes over the greater Horn of Africa region from 1961 to 2010. *Int. J. Clim.* **2014**, *34*, 1262–1277. [CrossRef]
12. Hashmi, M.Z.; Shamseldin, A.Y.; Melville, B.W. Statistical downscaling of precipitation: state-of-the-art and application of bayesian multi-model approach for uncertainty assessment. *Hydrol. Earth Syst. Sci.* **2009**, *6*, 6535–6572. [CrossRef]
13. Domínguez, M.; Romera, R.; Sánchez, E.; Fita, L.; Fernández, J.; Jiménez-Guerrero, P.; Montávez, J.; David, W.; Cabos, W.D.; Liguori, G.; et al. Present climate precipitation and temperature extremes over Spain from a set of high resolution RCMs. *Clim. Res.* **2013**, *58*, 149–164. [CrossRef]
14. Trenberth, K.E.; Jones, P.D.; Ambenje, P.; Bojariu, R.; Easterling, D.; Klein Tank, A.; Parker, D.; Rahimzadeh, F.; Renwick, J.A.; Rusticucci, M.; et al. Observations: Surface and atmospheric climate change. In *Climate Change 2007: The Physical Science Basis*; Contribution of Working Group I to the Fourth Assessment Report of the Intergovernmental Panel on Climate Change; Solomon, S., Qin, D., Manning, M., Chen, Z., Marquis, M., Averyt, K.B., Tignor, M., Miller, H.L., Eds.; Cambridge University Press: Cambridge, UK; New York, NY, USA, 2007.
15. Frias, M.D.; Minguez, R.; Gutierrez, J.M.; Mendez, F.J. Future regional projections of extreme temperatures in Europe: A non-stationary seasonal approach. *Clim. Chang.* **2012**, *113*, 371–392. [CrossRef]

16. Seneviratne, S.I.; Nicholls, N.; Easterling, D.; Goodess, C.M.; Kanae, S.; Kossin, J.; Luo, Y.; Marengo, J.; McInnes, K.; Rahimi, M.; et al. Changes in climate extremes and their impacts on the natural physical environment. In *Managing the Risks of Extreme Events and Disasters to Advance Climate Change Adaptation*; Field, C.B., Barros, V., Stocker, T.F., Qin, D., Dokken, D.J., Ebi, K.L., Mastrandrea, M.D., Mach, K.J., Plattner, G.-K., Allen, S.K., et al., Eds.; Cambridge University Press: Cambridge, UK, 2012; pp. 109–230.
17. Solomon, A.; Rao, P.; Rao, M.N. Statistical downscaling of daily temperature and rainfall data from global circulation models: In South Wollo zone, North Central Ethiopia. *J. Res. Sci. Tech.* **2013**, *2*, 27–39.
18. Ayalew, D.; Tesfaye, K.; Mamo, G.; Yitaferu, B.; Bayu, W. Outlook of future climate in Northwestern Ethiopia. *Agric. Sci.* **2012**, *3*, 608–624. [CrossRef]
19. Dile, Y.T.; Berndtsson, R.; Setegn, S.G. Hydrological response to climate change for Gilgel Abay river, in the Lake Tana basin—Upper Blue Nile basin of Ethiopia. *PLoS ONE* **2013**, *8*, e79296. [CrossRef] [PubMed]
20. Samuale, T.; Raj, A.; Girmay, G. Assessment of climate change impact on the hydrology of Geba catchment, Northern Ethiopia. *Am. J. Environ. Eng.* **2014**, *4*, 25–31. [CrossRef]
21. Rukundo, E.; Doğan, A. Assessment of climate and land use change projections and their impacts on flooding. *Pol. J. Environ. Stud.* **2016**, *25*, 2541–2551. [CrossRef]
22. Sayad, T.A.; Ali, A.M.; Kamel, A.M. Study the impact of climate change on maximum and minimum temperature over Alexandria, Egypt using statistical downscaling model (SDSAM). *Glob. J. Adv. Res.* **2016**, *3*, 694–712.
23. Ward, P.; Lasage, R. *Downscaled Climate Change Data from the HADCM3 and ECHAM5 Models on Precipitation and Temperature for Ethiopia and Kenya*; Institute for Environmental Studies, Vrije Universiteit: Amsterdam, The Netherlands, 2009.
24. Climate Change and Urban Vulnerability in Africa. Assessing Vulnerability of Urban Systems, Populations and Goods in Relation to Natural and Man-Made Disasters in Africa. 2011. Available online: http://www.cluva.eu/CLUVA_publications/CLUVA_Climate-change-and-vulnerability-of-African-cities-Research-briefs.pdf (accessed on 15 March 2016).
25. Birhanu, D.; Kima, H.; Jangb, C.; Park, P. Flood risk and vulnerability of Addis Ababa city due to climate change and urbanization. *Proc. Eng.* **2016**, *154*, 696–702. [CrossRef]
26. Arsiso, B.K.; Tsidu, G.M.; Stoffberg, G.H.; Tadesse, T. Influence of urbanization-driven land use/cover change on climate: The case of Addis Ababa, Ethiopia. *Phys. Chem. Earth* **2017**. [CrossRef]
27. World Bank. Enhancing Urban Resilience Addis Ababa, Ethiopia. 2015. Available online: https://www.gfdrr.org/sites/default/files/publication/Addis_Ababa_Resilient_cities_program.pdf (accessed on 14 August 2017).
28. Conway, D.; Mould, C.; Bewket, W. Over one century of rainfall and temperature observations in Addis Ababa, Ethiopia. *Int. J. Climatol.* **2004**, *24*, 77–91. [CrossRef]
29. Woldegerima, T.; Yeshitela, K.; Lindley, S. Characterizing the urban environment through urban morphology types (UMTs) mapping and land surface cover analysis: The case of Addis Ababa, Ethiopia. *Urban Ecosyst.* **2016**, *19*, 247–259. [CrossRef]
30. Kalnay, E.; Kanamitsu, M.; Kistler, R.; Collins, W.; Deaven, D.; Gandin, L.; Iredell, M.; Saha, S.; White, G.; Woollen, J.; et al. The NCEP/NCAR 40-year reanalysis project. *Bull. Am. Meteorol. Soc.* **1996**, *77*, 437–471. [CrossRef]
31. Schoof, J.T.; Pryor, S.C. Evaluation of the NCEP/NCAR reanalysis in terms of synoptic scale phenomena: A case study from the Midwestern USA. *Int. J. Clim.* **2003**, *23*, 1725–1741. [CrossRef]
32. McFarlane, N.A.; Scinocca, J.F.; Lazare, M.; Harvey, R.; Verseghy, D.; Li, J. *The CCCma Third Generation Atmospheric General Circulation Model*; CCCma Internal Report; University of Victoria: Victoria, BC, Canada, 2005; Available online: https://hal.archives-ouvertes.fr/hal-00304124/document (accessed on 19 October 2017).
33. Merryfield, W.J.; Lee, W.; Boer, G.J.; Kharin, V.V.; Scinocca, J.F.; Flato, G.M.; Ajayamohan, R.S.; Fyfe, J.C. The Canadian seasonal to interannual prediction system. Part I: Models and initialization. *Mon. Weather Rev.* **2013**, *141*, 2910–2944. [CrossRef]
34. Taylor, K.E.; Stouffer, R.J.; Meehl, G.A. An overview of Cmip5 and the experiment design. *Bull. Am. Meteorol. Soc.* **2012**, *93*, 485–498. [CrossRef]
35. Intergovernmental Panel on Climate Change. *Climate Change 2013: The Physical Science Basis*; Contribution of Working Group I to the Fifth Assessment Report of the Intergovernmental Panel on Climate Change; Stocker, T.F., Qin, D., Plattner, G.-K., Tignor, M., Allen, S.K., Boschung, J., Nauels, A., Xia, Y., Bex, V., Midgley, P.M., Eds.; Cambridge University Press: Cambridge, UK; New York, NY, USA, 2013.

36. Wilby, R.L.; Dawson, C.W.; Barrow, E.M. SDSM—A decision support tool for the assessment of regional climate change impacts. *Environ. Model. Softw.* **2002**, *17*, 145–157. [CrossRef]
37. Coulibaly, P.; Dibike, Y.B. Downscaling precipitation and temperature with temporal neural networks. *Am. Meteorol. Soc.* **2005**, *6*, 483–496. [CrossRef]
38. Wilby, R.L.; Harris, I. A framework for assessing uncertainties in climate change impacts: Low-flow scenarios for the River Thames, UK. *Water Res.* **2006**, *42*, W02419. [CrossRef]
39. Wily, R.L.; Dawson, C.W. SDSM 4.2—A decision support tool for the assessment of regional climate change impacts. User Manual. 2007. Available online: https://sdsm.org.uk/software.html (accessed on 15 December 2017).
40. Donat, M.G.; Alexander, L.V.; Yang, H.; Durre, I.; Vose, R.; Dunn, R.J.H.; Willett, K.M.; Aguilar, E.; Brunet, M.; Caesar, J.; et al. Updated analyses of temperature and precipitation extreme indices since the beginning of the twentieth century: The HadEX2 dataset. *J. Geophys. Res. Atmos.* **2013**, *118*, 1–16. [CrossRef]
41. Mahmood, R.; Babel, M.S. Future changes in extreme temperature events using the statistical downscaling model (SDSM) in the trans-boundary region of the Jhelum river basin. *Weather Clim. Extremes* **2014**, *5*, 56–66. [CrossRef]
42. Deque, M.; Dreveton, C.; Braun, A.; Cariolle, D. The ARPEGE/IFS atmosphere model: A contribution to the French community climate modelling. *Clim. Dyn.* **1994**, *10*, 249–266. [CrossRef]
43. Amadou, A.; Gado, D.A.; Seidou, O.; Seidou, S.I.; Ketvara, S. Changes to flow regime on the Niger River at Koulikoro under a changing climate. *Hydrol. Sci. J.* **2015**, *60*, 1709–1723. [CrossRef]
44. Choi, G.; Collins, D.; Ren, G.; Trewin, B.; Baldi, M.; Fukuda, Y.; Afzaal, M.; Pianmana, T.; Gomboluudev, P.; Huong, P.T.T.; et al. Changes in means and extreme events of temperature and precipitation in the Asia-Pacific network region, 1955–2007. *Int. J. Clim.* **2009**, *29*, 1906–1925. [CrossRef]
45. Mekonnen, D.F.; Disse, M. Analyzing the future climate change of Upper Blue Nile River basin using statistical downscaling techniques. *Hydrol. Earth Syst. Sci.* **2018**, *22*, 2391–2408. [CrossRef]
46. Gebrie, W.G.; Abate, B. Trend of lake evaporation considering climate change, the case of Lake Hawasa, Ethiopia. *Int. J. Sci. Res.* **2012**, *3*, 2319–7064.
47. Kebede, A.; Diekkruger, P.; Moges, S.A. An assessment of temperature and precipitation change projections using a regional and a global climate model for the Baro-Akobo Basin, Nile Basin, Ethiopia. *J. Earth Sci. Clim. Chang.* **2013**, *4*, 133. [CrossRef]
48. Worqlul, A.W.; Taddele, Y.D.; Ayana, E.A.; Jeong, J.; Adem, A.A.; Gerik, T. Impact of climate change on stream flow hydrology in headwater catchments of the Upper Blue Nile Basin, Ethiopia. *Water* **2018**, *10*, 120. [CrossRef]
49. Arsiso, B.K.; Tsidu, G.M.; Stoffberg, G.H.; Tadesse, T. Climate change and population growth impacts on surface water supply and demand of Addis Ababa, Ethiopia. *Clim. Risk Manag.* **2017**, *18*, 21–33. [CrossRef]
50. Teferi, E.; Abraha, H. Urban heat island effect of Addis Ababa City: Implications of urban green spaces for climate change adaptation. In *Climate Change Adaptation in Africa, Climate Change Management*; Filho, W.L., Belay, S., Kalangu, J., Menas, W., Munishi, P., Musiyiwa, K., Eds.; Springer: New York, NY, USA, 2017.
51. Feyissa, G.; Dons, K.; Meilby, H. Efficiency of parks in mitigating urban heat island effect: An example from Addis Ababa. *Landsc. Urban Plan.* **2014**, *123*, 87–95. [CrossRef]
52. Abebe, M.; Megento, T. The city of Addis Ababa from 'Forest City' to 'Urban Heat Island'. Assessment of urban green space dynamic. *J. Urban Environ. Eng.* **2016**, *10*, 254–262. [CrossRef]